

Nuclear effects in prompt photon production at the Large Hadron Collider

J. Jalilian-Marian¹, K. Orginos^{1,2} and I. Sarcevic¹

¹*Department of Physics, University of Arizona, Tucson, Arizona 85721*

²*RIKEN-BNL Research Center, Brookhaven National Laboratory, Upton NY 11973-5000*

Abstract

We present a detailed study of prompt photon production cross section in heavy-ion collisions in the central rapidity region at energy of $\sqrt{s} = 5.5$ TeV, appropriate to LHC experiment. We include the next-to-leading order radiative corrections, $O(\alpha_{em}\alpha_s^2)$, nuclear shadowing and the parton energy loss effects. We find that the nuclear effects reduce the invariant cross section for prompt photon production by 55% – 80% at LHC energies at $p_t = 3$ GeV. We discuss theoretical uncertainties due to parton energy loss and nuclear shadowing parameters. We show that the K-factor, which signifies the importance of next-to-leading order corrections, is large and has a strong p_t dependence.

1 Introduction

There has been a considerable theoretical and experimental interest in studying photon production in heavy-ion collisions at BNL's Relativistic Heavy Ion Collider (RHIC) and CERN's Large Hadron Collider (LHC) energies [1]. Photons produced in heavy-ion collisions provide an excellent probe of the properties of the dense matter, such as the quark-gluon plasma or the hot hadronic gas, produced after the collision. Due to the small cross sections of electromagnetic interactions, photons can escape the strongly interacting matter produced in the collision without further interactions.

Studying photon production at the RHIC and LHC energies is of special interest, as it has been suggested as an elegant signal for detecting the formation of a quark gluon plasma (QGP) in heavy-ion collisions [2]. However, photons can be produced at different stages of the heavy ion collision and thus have different origin. For example, photons can be produced at the early stages of the collision through QCD processes such as $qg \rightarrow q\gamma$ or they can be emitted from a thermalized quark gluon plasma or hadronic gas. Another source of produced photons is decay of hadrons such as pions and etas produced in the heavy ion collision [3]. Furthermore, different processes give the dominant contribution at different p_t 's. Therefore, it is quite difficult to make reliable predictions for the absolute number of photons produced in a heavy ion collision [4, 5].

Prompt photons are an important background to thermal photons in the low to intermediate p_t region and are dominant in the high p_t region. Therefore, it is extremely important to be able to calculate their production cross section reliably. Fortunately, one can use perturbative QCD in the high p_t region to calculate the prompt photon production cross section. In this work we study the production of high p_t ($p_t > 3$ GeV) prompt photons in heavy ion collisions. Prompt photons are produced either directly in the hard collisions of the partons inside the nuclei like $qg \rightarrow q\gamma$ or through bremsstrahlung of quarks and gluons produced in the hard collision such as $qg \rightarrow qg\gamma$. We include all next-to-leading order, $O(\alpha_{em}\alpha_s^2)$ QCD processes [6] as well as nuclear shadowing and medium induced parton energy loss effects. We discuss and estimate the theoretical uncertainties due to different choices of nuclear shadowing and energy loss parameters. We show that next-to-leading (NLO) corrections are large and must be included to make reliable predictions.

In section I we review the prompt photon production in hadronic collisions in next-to-leading order. Based on QCD factorization theorems, we write down the expression for prompt photon production and list the hard partonic processes involved. In section II we discuss the nuclear effects such as shadowing and energy loss involved in production of prompt photons in heavy ion collisions. In section III we present our results for the prompt photon production invariant cross section, $E \frac{d\sigma}{d^3p}$, at LHC energies and an estimate of the theoretical uncertainties due to variation of nuclear shadowing and energy loss parameters. We show that the effective K-factor, defined as the ratio of NLO to LO cross sections in heavy ion collisions is large and has a strong p_t dependence. This clearly shows the importance of including next-to-leading order contributions to prompt photon production. We conclude with a discussion of prospects for detecting nuclear effects by measuring prompt photons at LHC.

2 Prompt photon production in pQCD

Using factorization theorems and perturbative QCD, the inclusive cross section for prompt photon production in a hadronic collision can be written as a convolution of parton densities in a hadron with the hard scattering cross section and the parton to photon fragmentation function:

$$E \frac{d^3\sigma}{d^3p}(\sqrt{s}, p_T) = \int dx_a \int dx_b \int dz \sum_{i,j}^{partons} F_i(x_a, Q^2) F_j(x_b, Q^2) D^{\gamma/p}(z, Q_f^2) E_\gamma \frac{d^3\hat{\sigma}_{ij \rightarrow \gamma X}}{d^3p_\gamma} \quad (1)$$

where the $F_i(x, Q^2)$ is the i -th parton distribution in a nucleon, x_a and x_b are the fractional momenta of incoming partons, $D^{\gamma/p}(z, Q_f^2)$ is the photon fragmentation function with z being the fraction of parton energy carried by the photon. The parton-parton cross sections, $\frac{d^3\hat{\sigma}_{ij \rightarrow \gamma X}}{d^3p_\gamma}$, include all processes up to and including $O(\alpha_{em}\alpha_s^2)$, such as leading-order subprocesses:

$$\begin{aligned} q + \bar{q} &\rightarrow \gamma + g \\ q + g &\rightarrow \gamma + q \end{aligned} \quad (2)$$

and the next-to-leading order subprocesses,

$$\begin{aligned} q + q &\rightarrow q + q + \gamma \\ q + \bar{q} &\rightarrow q + \bar{q} + \gamma \\ q + q' &\rightarrow q + q' + \gamma \\ q + \bar{q} &\rightarrow q' + \bar{q}' + \gamma \\ q + \bar{q}' &\rightarrow q + \bar{q}' + \gamma \end{aligned} \quad (3)$$

We refer the reader to [6] for a complete list of all $O(\alpha_{em}\alpha_s^2)$ processes. A word of caution is in order here. To include all $O(\alpha_{em}\alpha_s^2)$ processes, it is necessary to include processes which formally look order $O(\alpha_{em}\alpha_s^3)$. This is because some of the terms in (3) have a divergence proportional to $1/\alpha_s$ which makes those processes $O(\alpha_{em}\alpha_s)$. This divergence comes from the quark and emitted photon being collinear. The reader is referred to [7] for a discussion of the collinear divergences.

The nucleon structure functions, $F_i(x, Q^2)$, and parton to photon fragmentation functions, $D^{p/\gamma}(z, Q_f^2)$, are also evaluated at the next-to-leading order. We use the MRS99 set for nucleon structure functions [8] and Bourhis et al. parameterization of the photon fragmentation functions [9]. Structure functions, fragmentation functions and the running coupling constant depend on the factorization, fragmentation and renormalization scales respectively which are usually taken to be the same and proportional to the photon transverse momentum p_t . Aurenche et al. [10] have studied the dependence of the prompt photon cross section on the choice of scale and have shown that the choice of $Q = p_t/2$ gives a very good description of prompt photon production in hadronic collisions. Therefore, we

will use $Q = p_t/2$ in our calculation. The running coupling constant $\alpha_s(Q^2)$, calculated to next-to-leading order, is given by

$$\alpha_s(Q^2) = \frac{12\pi}{(33 - 2N_f) \ln Q^2/\Lambda^2} \left[1 - \frac{6(153 - 19N_f) \ln \ln Q^2/\Lambda^2}{(33 - 2N_f)^2 \ln Q^2/\Lambda^2} \right] \quad (4)$$

where Q^2 is the renormalization scale, Λ is the QCD scale parameter and N_f is the number of flavors.

In Figure (1a) we illustrate the importance of including the next-to-leading order contributions by calculating the ratio of NLO to LO cross sections, the so-called K-factor. Clearly, the NLO corrections are large and p_t dependent. It would be useful to go even beyond the NLO to make sure that the higher order corrections are not even larger. It is, however, clear that a leading order calculation in the LHC kinematic region is meaningless since the next-to-leading order corrections are huge.

In Figure (1b)) we show an alternative definition of the K-factor defined as $K \equiv NLO/(LO + Brems.)$ sometimes used in the literature [4]. The main reason for this definition was inclusion of an incomplete set of Bremsstrahlung diagrams in previous works on prompt photon cross sections [4] and we show it here for comparison.

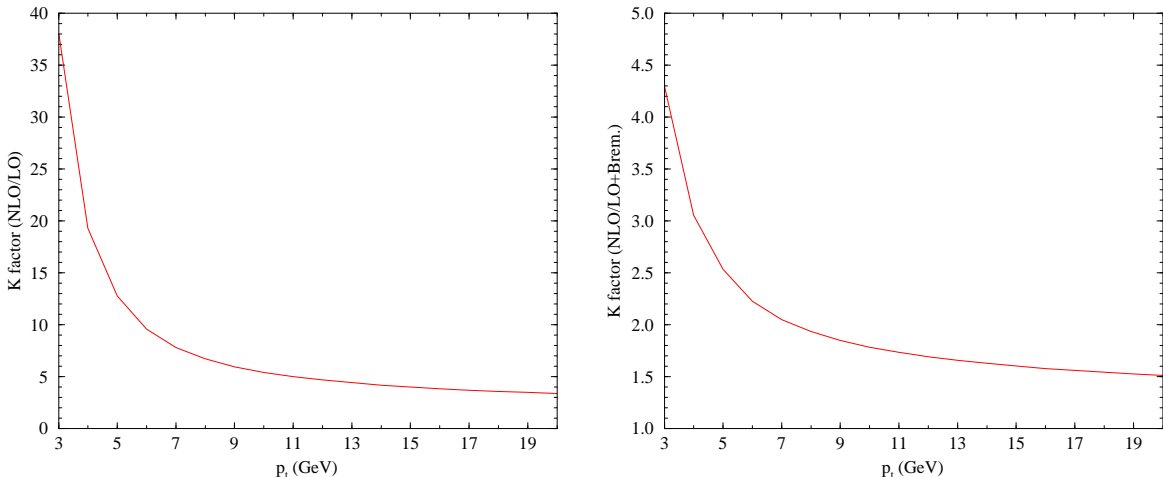


Figure 1: a) The hadronic K-factor defined as the ratio of NLO prompt photon cross section, $E \frac{d\sigma}{d^3p}$ to the LO cross section, and b) the K-factor defined as the ratio of NLO to the LO plus bremsstrahlung cross sections.

Also, one needs to resum certain logarithmic terms, of the form $\alpha_s \ln(1 - x_t)$ and $\alpha_s \ln x_t$ where $x_t \sim p_t/\sqrt{s}$ which become large in the very low and very high p_t region of phase space. These resummations are not very important for the range of p_t and \sqrt{s} that are considered in this work and will be neglected [11].

There is also an alternative approach to calculating prompt photon cross sections which uses the LO cross sections as well as LO structure and fragmentation functions. In order to

reproduce the experimental data in this approach, it is necessary to include a phenomenological parameter which is loosely identified as the “intrinsic” momentum of the initial state partons [12]. This intrinsic momentum is generated by the initial state radiation of quarks and gluons. There is however no theoretical calculation of these effects at the moment and one has to model them by generalizing the standard definitions of the parton distribution functions from $q(x, Q^2)$ and $G(x, Q^2)$ to $q(x, k_t^2, Q^2)$ and $G(x, k_t^2, Q^2)$. One then introduces a weight function, typically a Gaussian, with a width $\langle k_t^2 \rangle$ which represents the intrinsic transverse momentum of the initial state partons. Assuming some reasonable range in k_t , these intrinsic momenta are integrated over in the final result. One is then able to get a fairly good description of most of the experimental results.

It is important to realize that this intrinsic momentum k_t grows with energy and can be as large as $\sim 1 - 2$ GeV in fixed target experiments and ~ 5 GeV in the Tevatron [13]. Therefore, strictly speaking, it is not an intrinsic momentum. It is also process dependent and is not a universal parameter. Therefore, it is necessary to extract it from data in each experiment and can not be predicted. In our work, we will not follow this approach but instead we will use NLO perturbative QCD formalism because it seems theoretically more rigorous and self-consistent. NLO calculations give fairly good agreement with the experimental data at high energies where RHIC and LHC will operate. It is worth noting that there are also claims of inconsistencies among various data sets from different experiments at low energies [10, 13].

3 Prompt photon production in heavy ion collisions

To calculate the prompt photon production cross section in heavy ion collisions, we will use eq. (1) modified for nuclear effects:

$$E \frac{d^3\sigma^{AB}}{d^3p}(\sqrt{s}, p_t) = \int dx_a \int dx_b \int dz \sum_{i,j}^{\text{partons}} F_i^A(x_a, Q^2) F_j^B(x_b, Q^2) D_C^{\gamma/p}(z, Q_f^2) E_\gamma \frac{d^3\hat{\sigma}_{ij \rightarrow \gamma X}}{d^3p_\gamma} \quad (5)$$

where the $F_i^A(x, Q^2)$ is the i -th parton distribution in a nucleus and $D_C^{\gamma/p}(z, Q_f^2)$ is the photon fragmentation function in a nuclear environment. The partonic processes (a partial list) are given by (2, 3) as before. The nuclear structure function $F_i^A(x, Q^2)$ and fragmentation function $D_C^{\gamma/p}(z, Q_f^2)$ are not known to next-to-leading order, but rather they are NLO nucleon structure and fragmentation functions modified for nuclear effects. Strictly speaking, therefore, our calculation of prompt photon production in heavy ion collisions is not a next-to-leading order calculation but is the most complete calculation performed so far. Below, we will describe the nuclear modifications to structure functions and fragmentation functions in detail.

3.1 Impact parameter dependence

We assume that the parton density in a nucleus can be factorized in terms of the (usual) parton structure function modified by the medium effects, $F_i^A(x, Q^2)/A$, and the spatial distribution of partons at some impact parameter b , $T_A(b)$, i.e.

$$F_i^A(x, Q^2, b) \approx (F_i^A(x, Q^2)/A)T_A(b). \quad (6)$$

The nuclear thickness function, $T_A(b)$, is the number of nucleons per unit transverse area at fixed impact parameter. The spatial (impact parameter) integration over \vec{b}_1 that appears in the equation below gives the number of nucleon-nucleon collisions per unit of transverse area at fixed impact parameter, $T_{AA}(b)$, which is related to the nuclear density in the following way:

$$T_{AA}(b) = \int d^2 b_1 T_A(|\vec{b}_1|) T_A(|\vec{b} - \vec{b}_1|), \quad (7)$$

where the nuclear thickness function, $T_A(b)$, is the nuclear density integrated over the longitudinal size, i.e.

$$T_A(b) = \int_{-\infty}^{\infty} dz \rho_A(\sqrt{b^2 + z^2}). \quad (8)$$

The nuclear density that is most widely used in the literature is the Gaussian distribution

$$\rho(r) = \frac{A}{\pi^{3/2} a^3} e^{-r^2/a^2}, \quad (9)$$

where a is related to the charge radius of the nucleus, $\frac{3}{2}a^2 = \langle R_A^2 \rangle$. Functions $T_A(b)$ and $T_{AA}(b)$ can be obtained analytically and are given by

$$T_A(b) = \frac{A}{\pi a^2} e^{-\frac{b^2}{a^2}} \quad (10)$$

and

$$T_{AA}(b) = \frac{A^2}{2\pi a^2} e^{-\frac{b^2}{2a^2}}. \quad (11)$$

Alternatively, for A-A collisions we can take the nuclear density to be the Woods-Saxon distribution [7] given by

$$\rho(r) = \frac{n_0}{[1 + e^{(r-R_A)/d}]}, \quad (12)$$

where $n_0 \approx 0.17/fm^3$, R_A is the nuclear radius and $d = .54/fm$ is the “skin” thickness of this distribution. The density and the nuclear overlapping function are normalized so that $\int d^3 r \rho(r) = A$ and $\int d^2 b T_{AA}(b) = A^2$. For central collisions the overlapping function can be approximated by $T_{AA}(0) = A^2/\pi R_A^2$, which gives $T_{Au-Au}(0) = 29 mb^{-1}$ while $T_{Pb-Pb}(0) = 32 mb^{-1}$. Therefore, to get the number of prompt photons produced in a central collision at RHIC and LHC, one would need to multiply our cross sections by $29 mb^{-1}$ and $32 mb^{-1}$ respectively.

3.2 The Nuclear Shadowing Effect

Calculation of the prompt photons production cross section in nuclear collisions requires knowledge of the nuclear structure functions $F_i^A(x, Q^2)$. It is an experimental fact that $F_i^A(x, Q^2) \neq A F_i^N(x, Q^2)$ where $F_i^N(x, Q^2)$ is the free nucleon structure function. This modification has a strong x dependence and is due to having different nuclear effects in different region of phase space. At small values of x , for instance $x < \sim 0.07$, the nuclear structure function is less than nucleon structure function scaled by A . This is known as shadowing. As x grows bigger, nuclear structure functions get bigger than the free nucleon structure function. This is known as anti-shadowing. As x further increases, nuclear structure functions become less than the free nucleon ones again which is known as the EMC effect. In this section, we will concentrate on shadowing and anti-shadowing regions since those are the kinematic regions where the prompt photon production takes place. We refer the reader to [14] for a recent review of nuclear shadowing.

An intuitive explanation of nuclear shadowing and anti-shadowing effects depends on the reference frame of the nucleus. Of course, the physical observables such as structure functions can not depend on our choice of reference frame. However, working in different frames helps one identify the different physical mechanisms involved. In the rest frame of the nucleus and in perturbative QCD, shadowing is due to multiple interaction of the $q\bar{q}$ component of the photon wave function with the nucleus. The amplitude of $q\bar{q}A$ interaction is mostly imaginary at small x and multiple interactions of the pair with the nucleus introduces a phase difference between different amplitudes which leads to a destructive interference. This in turn reduces the nuclear cross section. In a non-perturbative description of shadowing, the photon is resolved in terms of its hadronic fluctuations which in turn multiply interact with the nucleus. The multiple interactions again reduce the nuclear cross sections due to destructive interference. In this frame, anti-shadowing at larger x is due to a large real part of the interaction amplitudes which interfere constructively with the imaginary part and lead to an enhancement of the nuclear cross section (structure functions).

In the infinite momentum frame where the nucleus is moving very fast, shadowing is caused by high parton density effects small x . The small x partons have a large longitudinal wavelength and can spatially overlap and recombine. These recombination effects reduce the nuclear parton number densities and hence the nuclear cross sections. Working in this frame enables one to treat nuclear shadowing and parton saturation in nucleons on the same footing due to the identical physical mechanism involved in both. Anti-shadowing is due to longitudinal momentum conservation (momentum sum rule) in this frame.

Even though there has been considerable amount of theoretical work done on nuclear shadowing and impressive progress made in understanding the physical principles of nuclear shadowing [14], we are far from having a precise and quantitative description of nuclear shadowing. In practice, one measures the nuclear structure functions in deep inelastic scattering of leptons on nuclei [15]. The measured structure functions are then used in nuclear collisions. The scale dependence of the nuclear structure functions is even less understood due to the limited range of Q^2 covered in fixed target experiments. Also, shadowing of

gluons is not well understood due to the fact that they can not be directly measured in DIS experiments. The working assumption is that high parton density effects are negligible and DGLAP evolution equations are valid in which case the gluon distribution function can be obtained from the scaling violation of the F_2 structure functions. This assumption, however, will break down at small values of x due to high parton density effects [16] and one will need to measure the gluon distribution function differently.

In this work we will use two different parameterizations of nuclear structure functions due to Benesh, Qiu, Vary [17] and Eskola et al. [18]. Both parameterizations fit the current experimental data quite well even though they are quite different. Also, since there are no experimental data at the small x , high Q^2 ($Q^2 > 1\text{GeV}^2$) region, any parameterization of nuclear structure functions in this region is subject to large uncertainties. This is somewhat important for RHIC but becomes crucial for LHC. An eA collider such as the proposed eRHIC is urgently needed and would greatly improve our knowledge of nuclear structure functions in the small x , high Q^2 region as well as reducing the theoretical uncertainties in the larger x region.

The parametrization of the nuclear shadowing function proposed by Benesh, Qiu and Vary is given by [17]

$$S(x, A) = \begin{cases} \alpha_3 - \alpha_4 x & x_0 < x \leq 0.6 \\ (\alpha_3 - \alpha_4 x_0) \frac{1+k_q \alpha_2 (1/x-1/x_0)}{1+k_q A^{\alpha_1} (1/x-1/x_0)} & x \leq x_0 \end{cases} \quad (13)$$

It gives a good description of all EMC, NMC and E665 data [15]. The parameters k_q , α_1 , α_2 , α_3 and x_0 are fitted to deep inelastic data for the ratio $F_2^A(x, Q^2)/F_2^D(x, Q^2)$ and can be found in [17]. In this parametrization, nuclear structure functions are independent of Q^2 and shadowing of gluons is assumed to be the same as quarks. A more recent parameterization of the nuclear structure function is that of Eskola et al. which also fits the existing experimental data quite well and is Q^2 dependent [18] and distinguishes between quark and gluon structure functions. We show the nuclear shadowing ratio defined as $S \equiv F_2^A/AF_2^N$ in Figure (2) using the parameterizations of both [17] and [18]. Clearly, the two are quite different although both fit the experimental data fairly well. This signifies the need for a high energy collider experiment such as eRHIC to improve on the current measurements of the nuclear structure functions.

In this work, we will use both parameterizations and investigate the dependence of prompt photon production cross sections on our choice of nuclear structure functions.

3.3 Medium induced parton energy loss effects

Another difference between hadronic and heavy ion collisions is in the multiplicity of the final state particles produced. In high energy heavy ion collisions and in central rapidities, the multiplicity of particles produced per unit rapidity is much larger than that in hadronic collisions. Therefore, many body effects such as secondary collisions, which are totally negligible in hadronic collisions become important in high energy heavy ion collisions. Another example is the medium induced energy loss. In hadronic collisions, since the number density of particles per rapidity produced is small, one can neglect the multiple

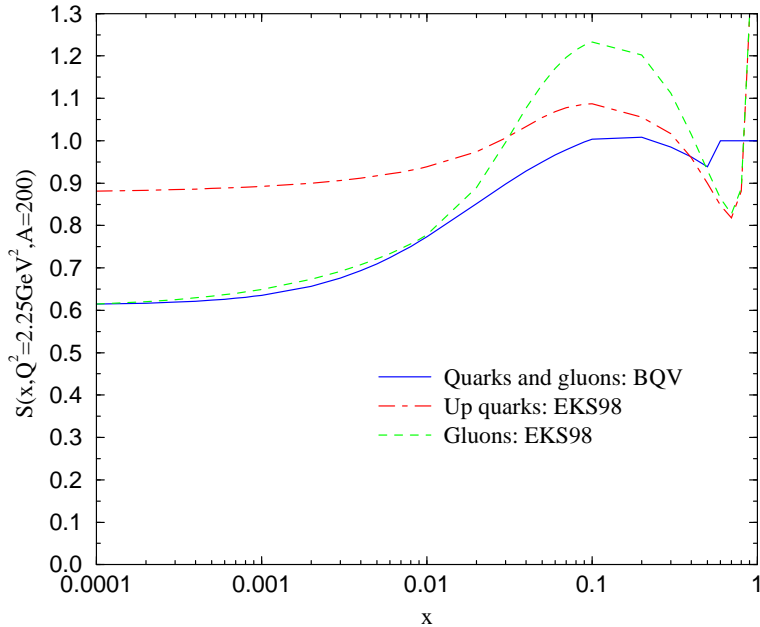


Figure 2: The nuclear shadowing ratio as parameterized by [17] (BQV) and [18](EKS98).

interactions of the produced partons with each other. On the other hand, in high energy heavy ion collisions, due to high multiplicities per unit rapidity, the multiple interactions of produced partons with each other can not be neglected. As a consequence of multiple interactions with the medium, produced particles can lose energy before hadronizing. This affects their energy and momentum spectrum.

Energy loss of energetic partons passing through a dense medium has been a hot topic lately [19]. There has been a considerable progress been made in understanding the different forms of the energy loss in different limits. It has been shown that, for a finite size medium, the parton energy loss is proportional to the its energy and therefore grows with energy. The current calculations of energy loss effects are done at the leading order $O(\alpha_s)$ and a next-to-leading order calculation is not presently available. Therefore we will use the leading order expressions in our calculation.

A rigorous treatment of energy loss effects in a heavy ion collision is extremely complicated and beyond the scope of this work. Rather, we will take a phenomenological approach to medium induced energy loss in nuclear collisions and use a model commonly used, due to Wang, Huang and Sarcevic [20], to estimate energy loss effects in high energy heavy ion collisions. In this model, it is assumed that the main effect of multiple interactions in the medium is to modify the photon fragmentation functions. In the central rapidity region, the produced parton in the hard collision is traversing the nuclear medium and losing energy as a result of multiple interactions with the deconfined medium. This parton will hadronize outside the nuclear medium but with a different energy which is less than its original energy.

In the energy loss model of Wang, Huang and Sarcevic [20], the parton to photon

fragmentation function, $zD_{\gamma/a}^0(z, Q_f^2)$, which gives the probability for a parton to fragment into a photon, is modified to include multiple scatterings of the fragmenting parton from the nuclear medium before it fragments. The nuclear fragmentation function $zD_{\gamma/a}(z, Q_f^2)$ is given in terms of the photon fragmentation function $zD_{\gamma/a}^0(z, Q_f^2)$ by [20]

$$zD_{\gamma/a}(z, \Delta L, Q_f^2) = \frac{1}{C_N^a} \sum_{n=0}^N P_a(n) \left[z_n^a D_{\gamma/a}^0(z_n^a, Q_f^2) + \sum_{j=0}^n \bar{z}_a^j D_{\gamma/g}^0(\bar{z}_a^j, Q_f^2) \right] \quad (14)$$

where $z_n^a = z / (1 - (\sum_{i=0}^n \epsilon_i^a) / E_t)$, $\bar{z}_j^a = z E_t / \epsilon_j^a$ and $P_a(n)$ is the probability that a parton of flavor a traveling a distance ΔL in the nuclear medium will scatter n times. It is given by

$$P_a(n) = \frac{(\Delta L / \lambda_a)^n}{n!} e^{-\Delta L / \lambda_a}, \quad (15)$$

and $C_N^a = \sum_{n=0}^N P_a(n)$. For the energy loss per unit distance ϵ_a , we take the energy dependent expression of Baier, Dokshitzer, Mueller, Peigne and Schiff [19], $\epsilon_a = \alpha_s \sqrt{\frac{\mu^2 E}{\lambda_a}}$, where E is the energy of the parton undergoing the multiple scatterings, λ_a is the parton inelastic mean free path and μ^2 represent a screening mass generated by the plasma and serves as an infrared cut off. The first term in Eq. (14) corresponds to the fragmentation of the leading parton a with reduced energy $E_t - \sum_{i=0}^n \epsilon_i^a$ after n gluon emissions and the second term comes from the j -th emitted gluon having energy ϵ_a^j . The nuclear fragmentation functions of quarks and gluons as defined in (14) are shown in Figure (3). For the photon fragmentation function, $zD_{\gamma/a}^0(z, Q_f^2)$, we use the parameterization of [9].

The parton to photon fragmentation functions in a nuclear medium are enhanced at small z and suppressed at large z as compared to the fragmentation functions in vacuum. This is due to the fact that high energy (high z) partons multiply scatter from the medium and lose their energy which shifts their energy fraction z to a smaller value.

As one goes to higher energies in heavy ion collisions, one probes smaller and smaller energy fractions z in the fragmentation functions. These fragmentation functions are fit to the experimental data and parameterized. However, the existing data does not cover the z ranges which will be explored by LHC. Therefore, the current parameterizations of parton to photon fragmentation functions are set equal to zero below some energy fraction $z_0 < \sim 0.01$. This is shown in Figure (3). In the kinematic region appropriate to LHC, however, one will need to know the fragmentation functions below this energy fraction. Therefore, we use both the standard (hadronic) fragmentation functions which are zero below z_0 and another parameterization which is identical to the standard one for $z > z_0$ but is set equal to a constant for $z < z_0$, i.e. $zD_{\gamma/g,g}^0(z, Q_f^2) = zD_{\gamma/g,g}^0(z = z_0, Q_f^2)$ for $z \leq z_0$.

In Figure (4) we show these modified fragmentation functions. We have checked that the difference between the two parameterizations leads to a negligible (< 1%) difference in the nuclear cross section. The reason is that the average z is not too small ($z > 0.1$) and thus the results are not sensitive to the variation of fragmentation functions in the small z

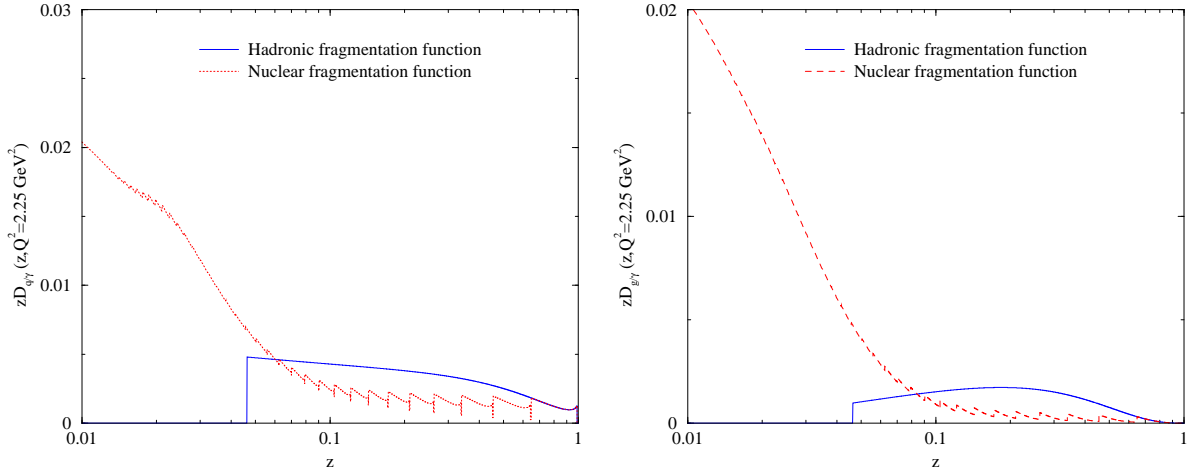


Figure 3: The photon fragmentation function, a) $zD_{\gamma/q}^0(z, Q_f^2)$ (solid line) [9] and the nuclear fragmentation function $zD_{\gamma/q}(z, Q_f^2)$ obtained using (14) (dashed line) and b) $zD_{\gamma/g}^0(z, Q_f^2)$ (solid line) [9] and the corresponding nuclear fragmentation function $zD_{\gamma/g}(z, Q_f^2)$ (dashed line).

region. Also, partonic cross sections at small z are power suppressed and do not contribute significantly.

We have studied the dependence of the prompt photon cross section on the screening mass. The screening mass, μ^2 , is generated by the deconfined quarks and gluons in the nuclear medium and has not been calculated in finite temperature QCD so far. It grows with the temperature of the medium and is commonly believed to be of order 1 GeV at RHIC and slightly higher at LHC. From Figure (5a) we note that starting with a very small μ^2 (small energy loss) and increasing it, the nuclear cross section decreases until it reaches a minimum after which increasing μ^2 any further will reduce the energy loss effects due to the finite energy of the fragmenting parton. This is in agreement with previous studies of energy loss effects in nuclear media [21].

The parton mean free path λ_a is also largely unknown and in principle depends on the parton species and the medium temperature. In this work, we treat μ^2 and λ_a as unknown parameters and show the dependence of our results on a physically reasonable variation of them. As seen in Figure (5b) and also Figure (5) in [22], this introduces a $\sim 25\%$ uncertainty at $p_t = 3$ GeV in both RHIC and LHC measurements of prompt photon cross sections.

4 Discussion

We show our results for the prompt photon cross section at LHC energies in Figures (6) and (8). We find nuclear effects at LHC to be striking. The nuclear cross sections are reduced by almost an order of magnitude at $p_t = 3$ GeV and 50% at $p_t = 20$ GeV. In Figure (6)

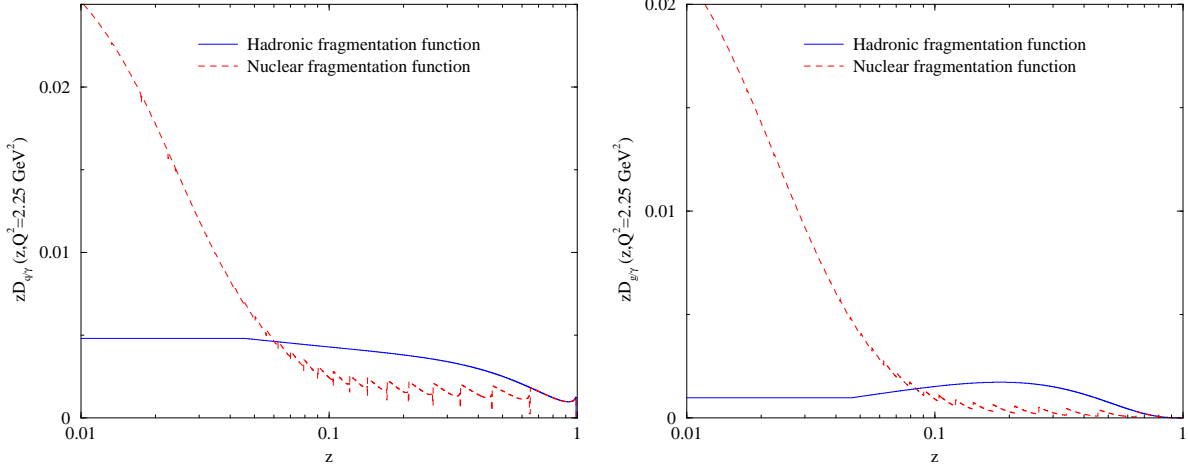


Figure 4: The modified photon fragmentation function a) $zD_{\gamma/q}^0(z, Q_f^2)$ (solid line) [9] and the nuclear fragmentation function $zD_{\gamma/q}(z, Q_f^2)$ obtained using (14) (dashed line) and b) $zD_{\gamma/g}^0(z, Q_f^2)$ (solid line) [9] and the corresponding nuclear fragmentation function $zD_{\gamma/g}(z, Q_f^2)$ (dashed line).

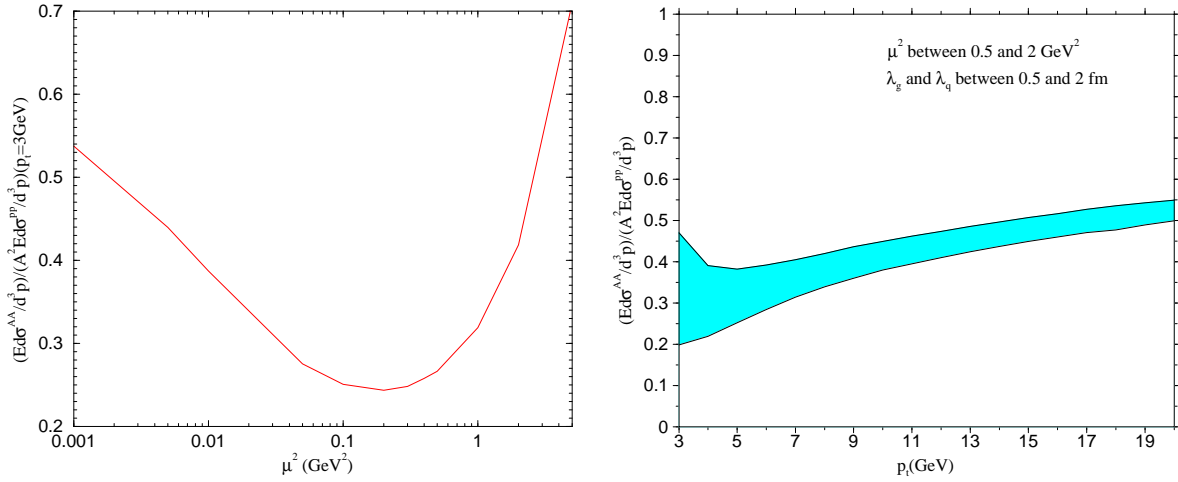


Figure 5: a) Prompt photon cross section in the central rapidity region at $\sqrt{s} = 5.5$ TeV as a function of μ^2 and b) the uncertainty in prompt photon cross section at $\sqrt{s} = 5.5$ TeV due to variation of energy loss parameters.

BQV parameterization of shadowing is used which is Q^2 independent. This reflects itself in the near constant ($\sim 30\%$) contribution of shadowing to the suppression of the nuclear cross section at all p_t . On the other hand, energy loss effects become smaller at larger p_t 's as expected ($\sim 50\%$ at $p_t = 3$ GeV and $\sim 20\%$ at $p_t = 20$ GeV).

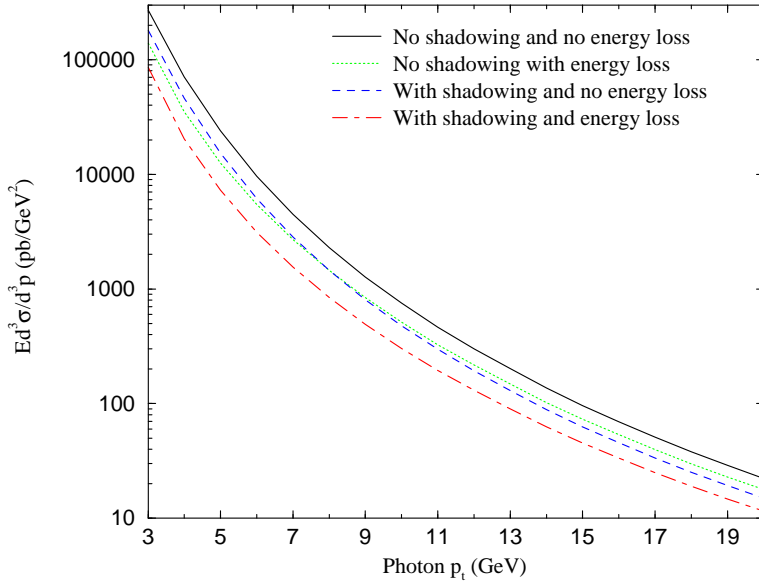


Figure 6: Prompt photon cross section in the central rapidity region at $\sqrt{s} = 5.5$ TeV using BQV shadowing [17].

To illustrate the importance of doing the full next-to-leading order calculation of prompt photon production at the LHC, we show the nuclear K -factors, defined as the ratio of NLO/LO and as the ratio of $NLO/(LO + \text{Brems.})$ cross sections in Figure (7).

In Figure (8) we use both the BQV [17] and the EKS98 [18] parameterization of shadowing. The EKS98 parameterization is Q^2 dependent and distinguishes between quark and gluon shadowing while the BQV parameterization is Q^2 independent and does not distinguish between quark and gluon shadowing. The difference at low p_t ($p_t \sim 3$ GeV) is small, about 4% while at $p_t = 20$ GeV it is about 20%. This is mainly due to the Q^2 dependence of EKS98 parameterization.

It is clear that nuclear effects at LHC are significant and should be easily detectable. Nuclear shadowing effects are large and need to be better understood. In Figure (9) we show the rescaled nuclear cross section using the BQV and EKS98 nuclear shadowing. The difference between the two parameterizations of nuclear shadowing is huge at large p_t .

The current parameterizations of nuclear shadowing in the kinematic region appropriate to LHC are extrapolations from low energy fixed target data and subject to large uncertainties. A precise quantitative knowledge of the nuclear structure functions at the small x , large Q^2 kinematic region is crucial. A lepton nucleus collider such as eRHIC is urgently needed.

Energy loss effects are also large. Whether one can reliably extract the energy loss

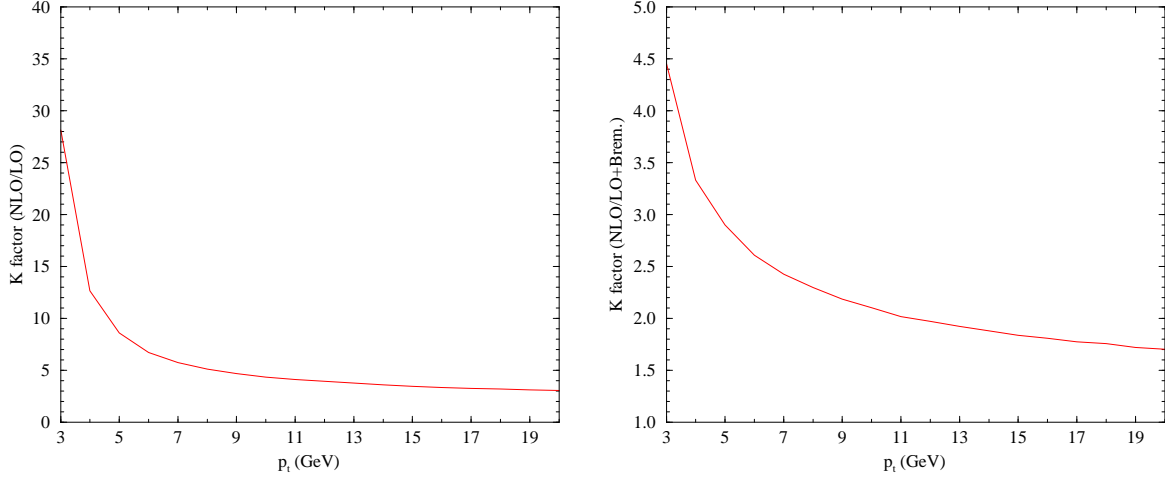


Figure 7: a) The nuclear K-factor defined as the ratio of NLO prompt photon cross section in heavy-ion collisions, $E \frac{d\sigma}{d^3 p}$, to the LO cross section and b) the K-factor defined as the ratio of NLO to the LO plus bremsstrahlung cross sections.

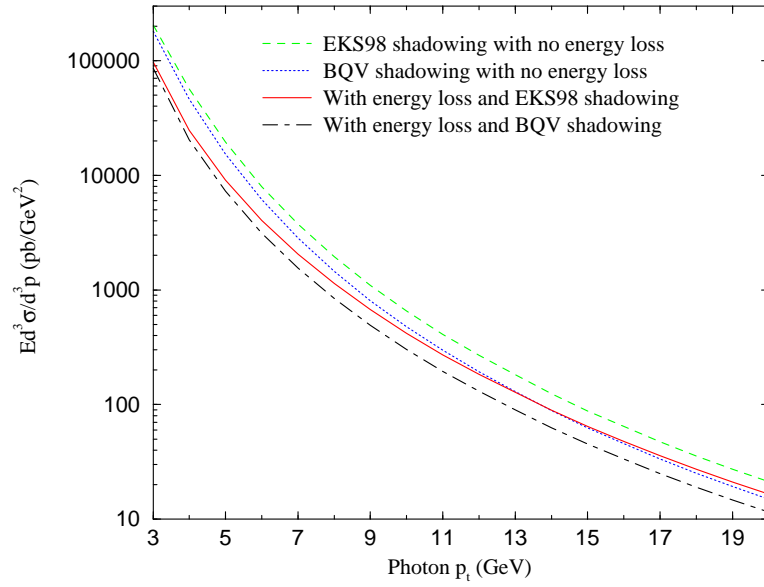


Figure 8: Prompt photon cross section in the central rapidity region at $\sqrt{s} = 5.5$ TeV obtained with EKS98 shadowing and without parton energy loss (dotted line), with parton energy loss (dashed line), with BQV shadowing and no parton energy loss (solid line) and with energy loss (dot-dashed line).

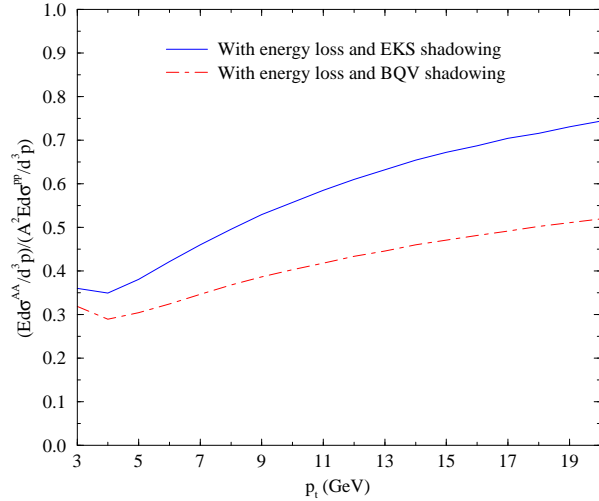


Figure 9: The rescaled prompt photon cross section in the central rapidity region at $\sqrt{s} = 5.5$ TeV using BQV [17] and EKS98 [18] shadowing.

parameters μ^2 and λ_a will depend on our precise knowledge of nuclear structure functions and also on the precision of the prompt photon measurements at RHIC and LHC. Distinguishing prompt photons from those coming from decays of pions and eta's is notoriously difficult. Also, one expects that the calculation of the ratio of prompt photons to pions would reduce some of theoretical uncertainties such as scale dependence and intrinsic k_t effects, thus making the NLO calculation even more reliable [23]. We intend to calculate this ratio in the near future [24].

Acknowledgments

We would like to thank P. Aurenche and M. Werlen for providing us with the fortran routines for calculating double differential distributions for photon production in hadronic collisions and for many useful discussions. J. J-M would like to thank S. Jeon, M. Tannenbaum and X-N. Wang for many helpful discussions. J. J-M is grateful to LBNL nuclear theory group for the use of their computing resources. This work was supported in part through U.S. Department of Energy Grants Nos. DE-FG03-93ER40792 and DE-FG02-95ER40906.

References

- [1] See for example, the proceedings of the XIVth International Conference on Ultrarelativistic Nucleus-Nucleus Collisions (Quark Matter 1999), *Nucl. Phys.* **A661** (1999).
- [2] L. McLerran and T. Toimela, *Phys. Rev.* **D31**, 545 (1985); E.V. Shuryak, *Phys. Lett.* **B78**, 150 (1978); *Phys. Rep.* **61**, 72 (1980).
- [3] J. Kapusta, P. Lichard and D. Seibert, *Phys. Rev.* **D44**, 2774 (1991); Erratum: *ibid.* **D47**, 4171 (1993).

- [4] N. Hammon, A. Dumitru, H. Stocker and W. Greiner, *Phys. Rev.* **C57**, 3292 (1998); A. Dumitru and N. Hammon, hep-ph/9807260.
- [5] D.K. Srivastava, nucl-th/9911047; D.K. Srivastava and B. Sinha, nucl-th/0006018.
- [6] P. Aurenche, R. Baier, M. Fontannaz and D. Schiff, *Nucl. Phys.* **B297**, 661 (1988).
- [7] P. Aurenche, P. Chiappetta, M. Fontannaz, J. Guillet and E. Pilon, *Nucl. Phys.* **B399**, 34 (1993).
- [8] A.D. Martin, R.G. Roberts, W.J. Stirling and R.S. Thorne, *Eur. Phys. J.* **C14**, 133 (2000).
- [9] M. Gluck, E. Reya and A. Vogt, *Phys. Rev.* **D48**, 116 (1993); Erratum: *ibid.* **D51**, 1427 (1995); L. Bourhis, M. Fontannaz and J.Ph. Guillet, *Eur. Phys. J.* **C2**, 529 (1998).
- [10] P. Aurenche, M. Fontannaz, J.Ph. Guillet, B. Kniehl, E. Pilon and M. Werlen, *Eur. Phys. J.* **C9**, 107 (1999).
- [11] G. Sterman and W. Vogelsang, hep-ph/0011289 and references therein.
- [12] J. Houston, E. Kovacs, S. Kuhlmann, H. Lai, J. Owens and W. Tung, *Phys. Rev.* **D51**, 6139 (1995); L. Apanasevich et al., *Phys. Rev.* **D59**, 074007 (1999); *ibid.* **D63**, 014009 (2001).
- [13] Report of the working group on photon and weak boson production, hep-ph/005226.
- [14] M. Arneodo, *Phys. Rep.* **240**, 301 (1994).
- [15] M.R. Adams, et al., *Phys. Rev. Lett.* **68**, 3266 (1992).
- [16] L. McLerran and R. Venugopalan, *Phys. Rev.* **D49**, 335 (1994); **D49**, 2233 (1994); J. Jalilian-Marian, A. Kovner, A. Leonidov and H. Weigert, *Phys. Rev.* **D59**, 034007 (1999); *ibid.* **D59**, 014015 (1999); J. Jalilian-Marian and X-N. Wang, *Phys. Rev.* **D60**, 054016 (1999); hep-ph/0005071; Z. Huang, H.J. Lu and I. Sarcevic, *Nucl. Phys.* **A637**, 70 (1998).
- [17] C.J. Benesh, J. Qiu and J.P. Vary, *Phys. Rev.* **C123**, 1015 (1994).
- [18] K. Eskola, V. Kolhinen and P. Ruuskanen, *Nucl. Phys.* **B535**, 351 (1998); K. Eskola, V. Kolhinen and C. Salgado, *Eur. Phys. J.* **C9**, 61 (1999).
- [19] R. Baier, Y. Dokshitzer, A. Mueller, S. Peigne and D. Schiff, *Nucl. Phys.* **B483**, 291 (1997); *ibid.* **B484**, 265 (1997); R. Baier, D. Schiff and B.G. Zakharov, hep-ph/0002198.
- [20] X-N. Wang, Z. Huang and I. Sarcevic, *Phys. Rev. Lett.* **77**, 231 (1996); X-N. Wang and Z. Huang, *Phys. Rev.* **C55** 3047 (1997).
- [21] X-N. Wang, *Phys. Rev.* **C58**, 2321 (1998).
- [22] J. Jalilian-Marian, K. Orginos and I. Sarcevic, hep-ph/0010230, to appear in *Phys. Rev. C*, March 2001.
- [23] M. Tannenbaum, private communication.
- [24] J. Jalilian-Marian, K. Orginos and I. Sarcevic, in preparation.